Polarization-Driven Stark Shifts in Quantum Dot Luminescence from Single CdSe/oligo-PPV Nanoparticles

ARTICLE *in* NANO LETTERS · APRIL 2010

Impact Factor: 13.59 · DOI: 10.1021/nl1001789 · Source: PubMed

NANO LETTERS

pubs.acs.org/NanoLett

Polarization-Driven Stark Shifts in Quantum Dot Luminescence from Single CdSe/oligo-PPV Nanoparticles

K. T. Early, P. K. Sudeep, T. Emrick, and M. D. Barnes*

Department of Chemistry and Department of Polymer Science and Engineering, University of Massachusetts, Amherst, Amherst, Massachusetts 01003

ABSTRACT We demonstrate polarization-induced spectral shifts and associated linearly polarized absorption and emission in single CdSe/oligo-(phenylene vinylene) (CdSe/OPV) nanoparticles. A mechanism for these observations is presented in which charge separation from photoexcited ligands results in a significant Stark distortion of the quantum dot electron/hole wavefunctions. This distortion results in an induced linear polarization and an associated red shift in band-edge photoluminescence. These studies suggest the use of single quantum dots as local charge mobility probes.

KEYWORDS Stark shift, polarization, quantum dots, single molecule

Understanding energy and charge exchange processes in nanostructured materials is critically important for development of high-efficiency optoelectronic devices. Surface-functionalized quantum dot (QD) systems with semiconducting organic materials offer an interesting material format to explore such interactions, where the molecular architecture and choice of ligands can be used to manipulate spatial, temporal, and spectral properties of the QD luminescence.[1−3] Recent studies have shown that ligands with electron-donating character can have profound effects on fluorescence intensity fluctuations (blinking) and photostability in isolated QD systems.[4,5] In similar systems where surfactants have been used to facilitate charge transfer between nanocrystals and organics, strong modification of QD photoluminescence intensity fluctuations (blinking suppression) have been observed.[6] These observations seem to point to a common mechanistic origin; namely that enhanced charge density near the surface of the QD can profoundly affect QD luminescence properties. However, definitive evidence linking excess surface charges to modified QD luminescence has not been shown.

In this letter, we report our observation of polarization-resolved spectral shifts ($\Delta E \approx -70$ meV) from individual CdSe QDs surface-functionalized with monodisperse oligo-(phenylene vinylene) ligands (CdSe/OPV). We show that both the observed spectral shift and linear polarization can be quantitatively described by a screened electrostatic (Stark) polarization of the QD electron−hole wavefunction from a single point-charge, providing compelling evidence for a charge-separation mechanism for excited state quenching in the organic surface ligands. These observations suggest the potential of using emission energy and luminescence polarization from single CdSe nanocrystals as local probes of mobility of nearby charge carriers.

The CdSe/OPV NP system is a hybrid inorganic/semiconducting organic structure which appears to retain photophysical properties of both the QD core and the organic ligand. Fluorescence emission spectra from individual CdSe/OPV nanoparticles (NPs) are characterized by an almost complete extinction of the organic ligand fluorescence, blinking suppression, and an enhanced spectral stability relative to TOPO-capped QDs.[3] Greater than 99% of the fluorescence intensity is carried by the band-edge luminescence of the QD. Observation of photon antibunching from single CdSe/OPV NPs (>75% modulation at $\Delta\tau = 0$) confirmed that the novel polarization and blinking suppression derives from surface-modified QD photophysics and gives further evidence for strong OPV-QD interactions resulting in single-fluorophore behavior.[8] In addition, we recently reported a surprising linear polarization in both absorption and emission from individual CdSe/OPV NPs.[9,10] While linear polarized luminescence has been observed in CdSe nanorods[2] (where strong exciton confinement exists in only one dimension) or in prolate nanocrystals at low temperature (where the shape distortion lifts the degeneracy of orthogonal X-Y Bloch components in the QD wavefunctions),[1] the CdSe/OPV system preserves a spherical symmetry as implied by atomic force microscopy (AFM) and dynamic light scattering (DLS) structural studies. We speculated that the observed linear dichroism in absorption ($\langle M \rangle \approx 0.6$) and distinct linear dipole emission patterns derived from an enhanced absorption cross section of the hybrid system at excitation polarizations that overlap with the ligand conjugation axis. Exciton dissociation within the

* Author to whom correspondence should be addressed.
Received for review: 01/18/2010
Published on Web: 00/00/0000

DOI: 10.1021/nl1001789 | *Nano Lett.* **XXXX,** *xxx,* 000–000

organic ligand, followed by electron trapping near the QD surface[9] offered an attractive heuristic explanation in that it qualitatively accounted for the quenching of the organic luminescence, and the linear dipole character.

This mechanism should have a clear experimental signature in the alteration of electron and hole energies from the Stark interaction from the electric field generated from a point-charge near the QD surface such that the apparent recombination energy is lowered. Here we report on measurements of spectral shifts of band-edge luminescence from single CdSe/OPV NPs correlated with a specific polarization angle of the excitation source. We observed red shifts greater than 70 meV (peak to peak) for excitation polarizations corresponding to maximum luminescence intensity, compared to the ~10 meV random spectral diffusion observed in ZnS-capped quantum dots of similar core radius. These observations are supported by perturbation calculations of the Stark-induced wavefunction distortion, spectral shifts, and induced linear polarization. First-order corrections to the QD $1S_e$ electron and $1S_{3/2,M}$ hole energies and wavefunctions arising from a trapped charge at the QD surface account quantitatively for both the spectral shifts and polarization anisotropy observed in single CdSe/OPV NPs. These combined results strongly support an exciton dissociation mechanism in the organic ligands, where the electric field from the electron near the QD surface drives a Stark shift of the QD band-edge energy, as well as a strong linear polarization along the axis connecting the excess charge and the QD center. Modulation of the pump polarization acts as the initiator of the Stark field, which appears as a slowly varying DC field on the spectral integration and polarization rotation time scales required for single-particle spectral measurements.

Figure 1A shows a schematic of the experimental setup. Samples (see Supporting Information for sample preparation details) were excited using wide-field epi-illumination using a lens to focus a continuous wave 405 nm diode laser at the back aperture of a 1.4NA, 100× microscope objective. Laser light transmitted through the sample was focused through a linear polarizer (POL) onto a photodiode (PD) to record the laser polarization (rotated using a half-wave ($\lambda/2$) plate); this technique was reported by Jung et al.[11] for interrogating rotational dynamics of chromophores in confined matrices. In these experiments, the $\lambda/2$ plate was rotated using a mechanical rotation stage (Newport 8401 with Picomotor driver), limiting polarization modulation speeds to $\sim 2\pi$ rad/7 s. A 435 nm long-pass dichroic mirror (DC) and 530 nm long-pass emission filter were used to filter out residual laser scatter and sample autofluorescence. Particle fluorescence was collected through the same objective, focused using a 200 mm tube lens, and routed to either a high-speed imaging charge-coupled device (CCD) or to a spectrograph/high-aspect ratio CCD for spectral measurements. In all cases, single QD photoluminescence intensity scaled linearly with excitation intensity, ensuring that we avoided any complications arising from multiexciton generation. Spectra were

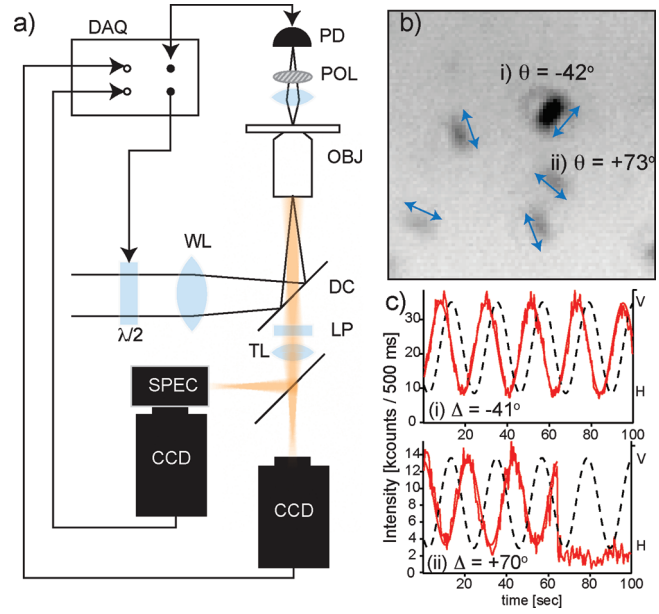

FIGURE 1. (a) Experimental setup. See text for details. Polarization modulation is controlled via half wave plate (l/2) and monitored in transmission through a POL and PD. Polarization rotation and monitoring are synced with camera exposures via DAQ board. (b) Summed widefield image of CdSe/OPV under slight defocusing; arrows show approximate transition dipole orientation. Fit orientation for particles (i) and (ii) are −42 and +73°, respectively. (c) Polarization trajectories for particles (i) and (ii) along with laser polarization (dashed line). Phase offsets are given, showing good agreement with widefield results.

recorded using 2 s exposures with a resolution of 0.6 meV/pixel. We used a multichannel data acquisition (DAQ) board (National Instruments) to synchronize the CCD camera exposures with polarization measurements.

Figure 1B shows a sample widefield image of several CdSe/OPV NPs under slight (~600 nm) defocusing. Defocused emission pattern imaging is now a commonly used method for the determination of molecular transition dipole moment orientation; fluorescent systems with single (linear) dipole character show distinct patterns defined by the dipole orientation in θ and ϕ.[12−14] As previously observed,[9] the emission from single CdSe/OPV NPs show the characteristic dipole pattern for an in-plane linear dipole (signified by arrows for particles i and ii). Because we are interested only in the in-plane orientation in these measurements, we used a simplified elliptic Gaussian fitting routine (see Supporting Information) yielding emission dipole moments −42 and +73° with respect to the vertical polarization axis for molecules (i) and (ii), respectively. Defocused emission patterns were fit after summing all fluorescence images and subtracting background pixel counts. Differences in particle intensity in the widefield image arise from fluorescence intermittency and bleaching during the experiment.

For these same particles, fluorescence intensity trajectories were recorded under rotating pump polarization, showing strong polarization anisotropy in absorption, also consistent with our earlier reports.[9] Figure 1C shows polarization

DOI: 10.1021/nl1001789 | *Nano Lett.* **XXXX,** *xxx,* 000–000

trajectories for the two particles, along with the laser polarization (ranging from vertical to horizontal, dashed lines). Particles (i) and (ii) modulate with phase offset angles of −41 and +70° respectively, which we obtain by comparing the phase offset term Δ in a fit to $A + B\cos^2(\omega x + \Delta)$ for the transmitted laser polarization and the CdSe/OPV fluorescence anisotropy signal. Abrupt photobleaching is evident in the fluorescence signal for particle (ii), evidence of the single-emitter nature of CdSe/OPV NPs. The small difference in orientation determination from the two methods could arise from error in the image fitting procedure, which we estimate to be 2−5° depending on fluorescence signal levels. However, small offsets in the absorption and emission transition dipoles of organic dyes have been reported in similar studies and were attributed to inverted lab-frame molecular conformations on the sample surface.[15] We note here that significant information could be gained in the temporal response from single particles to polarization modulation on fast time scales (comparable to the relaxation time of the charge separated organic state), analogous to amplitude modulation experiments. Future experiments utilizing faster polarization modulation hardware (i.e., computer-controlled electro-optic modulators) are planned to probe this temporal response.

Figure 2A shows peak emission energies from a single CdSe/OPV NP (top, red lines/markers) and a CdSe/ZnS QD (middle, blue line) as a function of slowly varying laser polarization (bottom) obtained using the same microscope configuration to collect sequential emission spectra (spectral trajectories) from single NPs. Similar experimental setups have been used to study DC Stark shifts,[16] zero-phonon lines,[17] and discrete spectral events[18,19] in single QDs at low temperature, and irreversible blue shifting[20,21] at room temperature. Sequential spectra were fit to a single Lorentzian function using an automated routine to determine center position, amplitude, and width and data were manually checked to exclude contributions from particles showing irreversible blue shifting. For both particles, the average emission energy is superimposed on the trajectory, and the average energy of the CdSe/ZnS QD has been red shifted by 70 meV for easier comparison with CdSe/OPV. The emission energy fluctuations of CdSe/ZnS appear largely insensitive to laser polarization and exhibit a narrow range of values, characteristic of normal spectral diffusion in single nanocrystals.[22] A histogram of peak energies (see Supporting Information) gives an average emission peak $\varepsilon_{avg} = 2.086$ eV with a full width half-maximum (fwhm) of 12.5 ± 0.3 meV, consistent with previous reports.[23] In contrast CdSe/OPV shows large, reversible fluctuations in emission ($\varepsilon_{avg} =$ 2.209 eV, fwhm = 28 ± 3 meV). Figure 2B shows two full emission spectra with Lorentzian fits from the CdSe/OPV trajectory in Figure 2a at the positions marked ($t = 140$ s and $t = 180$ s), corresponding to approximately orthogonal excitation polarizations. The spectral cutoff at the low-energy edge of the spectrum is the result of the finite wavelength

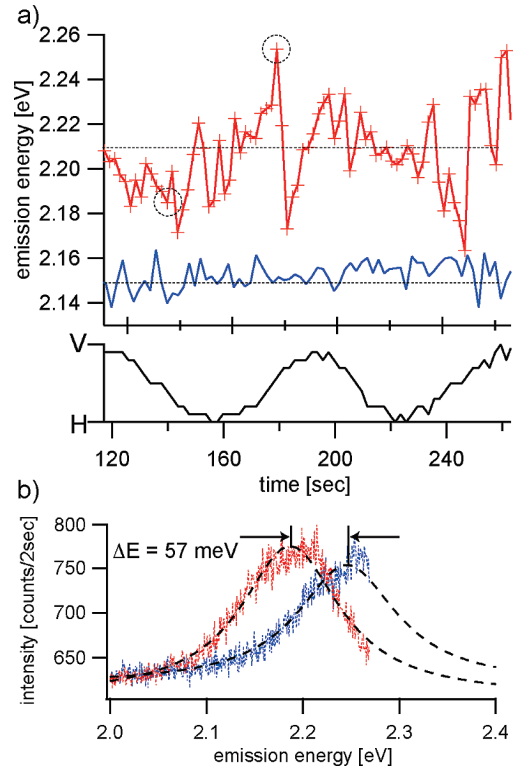

FIGURE 2. (a) Peak emission energy versus laser polarization for a CdSe/OPV NP (top, red lines/markers) and a CdSe/ZnS QD (middle, blue), with dashed lines showing average energy. Laser polarization is shown on bottom. CdSe/ZnS energies are offset by 70 meV for comparison. (b) Emission spectra for CdSe/OPV at the positions marked in (a) corresponding to orthogonal laser polarization with Lorentzian fits. Peak emission shift is 57 meV.

range of the spectrograph/CCD array. The measured spectral shift between the two peaks is 57 meV with shifts as large as 70 meV observed in single CdSe/OPV NPs. Shifts of this magnitude are seen only under rotating laser polarization, which otherwise undergo standard spectral diffusion. Larger amplitude shifts are present in the CdSe/OPV trajectory in Figure 2a that do not occur at orthogonal excitation polarizations. We speculate that these sudden jumps arise from nonradiative recombination of organic excitons, which complicates the analysis of the experimental dependence of the Stark shift on pump polarization. The broadened spectral width can be attributed to charge dynamics that are fast on the time scale of polarization modulation, which we discuss below.

DC Stark Effect Mechanism. In previous work, we proposed that linear dichroism in CdSe/OPV NPs derived from the formation of trapped surface charges.[9] Excitations generated in the coordinated organics attached to the surface of the CdSe QD are strongly polarized along the conjugation axis of the ligand. Because of the alignment of CdSe electron/hole levels and OPV HOMO−LUMO gap, the proximal CdSe QD acts as an electron sink,[24,25] generating a driving force for dissociation of the organic exciton and transfer of the electron to the QD surface. This results in a long-lived (~800 μs) polaron in the OPV ligand.[26] The

DOI: 10.1021/nl1001789 | *Nano Lett.* **XXXX,** *xxx,* 000–000

resulting electron trapped near the QD surface generates an electric field which perturbs the envelope wavefunctions of the photogenerated electron and hole in the quantum dot. This perturbation mixes the lowest-lying $1S_e$ and $1P_e$ electron levels as well as the (highest-lying) $1S_{3/2}$ and $1P_{3/2}$ hole states, effectively lowering the QD band edge energy.

To model the spectral shifts and linear polarization, we computed the first order Stark corrections to the $1S_e$ and $1S_{3/2,M}$ electron/hole wavefunctions[27] using an operator adaption of the Coulomb interaction energy function between a fixed point charge q at a distance S from the QD surface, and the electron/hole within the QD, as discussed by Wang.[28] The relevant matrix element for the fixed-charge/electron interaction is

$$\langle V_e^{(1)} \rangle = \frac{qe}{4\pi\varepsilon_0 S^2} \frac{3}{(2+\gamma)} \langle 1S_e | r\cos[\theta] | 1P_e \rangle \qquad (1)$$

where γ is a QD-size dependent screening constant (taken here to be equal to 5.5 from Wang et al.[29]). The correction to the $1S_e$ energy was computed as

$$\delta_{1S_e} = -\frac{\langle V_e^{(1)} \rangle^2}{\Delta E_{1Se,1Pe}} \qquad (2)$$

using a value of 0.42 eV for the energy difference between $1S_e$ and $1P_e$ electron levels. The hole states are each 4-fold degenerate, corresponding to $M = \pm 3/2, \pm 1/2$ projection of spin angular momentum onto the z-axis. The $1S_{3/2,M}$ wavefunctions therefore take a slightly different form, depending on the choice of M; in general, these states contain higher spherical harmonics, and the interaction energies require two integrals

$$\langle V_h^{(1)} \rangle = -\frac{qe}{4\pi\varepsilon_0 S^2} \frac{3}{(2+\gamma)} \langle 1S_{3/2,M} | r\cos[\theta] | 1P_{3/2,M} \rangle$$

$$\langle V_h^{(3)} \rangle = -\frac{qe}{8\pi\varepsilon_0 S^4} \frac{7}{(4+3\gamma)} \langle 1S_{3/2,M} | r^3(-3\cos[\theta] + 5\cos^3[\theta]) | 1P_{3/2,M} \rangle \qquad (3)$$

The corrections to the hole wavefunction and energy were computed using a value of 0.05 eV for the energy difference between $1S_{3/2}$ and $1P_{3/2}$ hole levels. Figure 3 shows the calculated magnitude of the Stark shift as a function of charge distance from the surface for a QD. Comparison with our experimental results suggests a cycle-averaged distance of ~1.4 nm separating the charge and the QD surface.

Figure 4 shows the computed $1S_e$ and $1S_{3/2,M=+3/2}$ electron and hole states perturbed by a fixed electron 1 nm from the dot surface. Qualitatively, these results are similar to those reported by Wang,[28] although in our calculations the distortion of the hole state appears smaller. Physically, the distor-

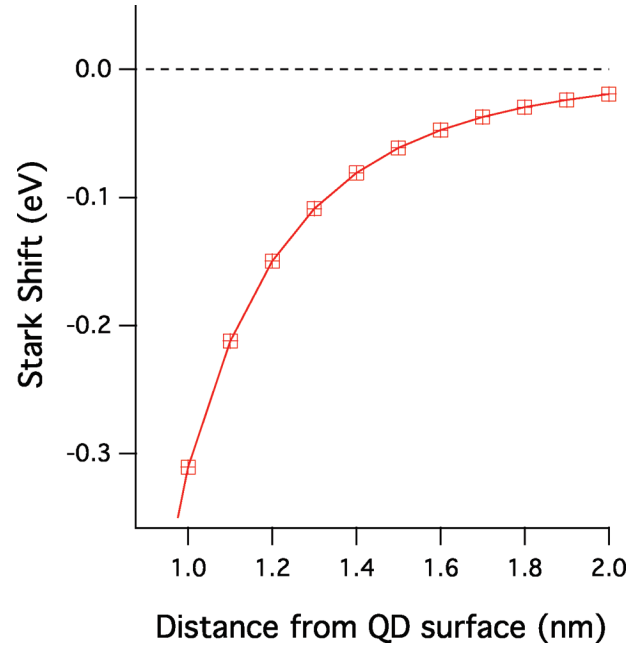

FIGURE 3. Stark shift magnitude as a function of charge proximity to the QD surface.

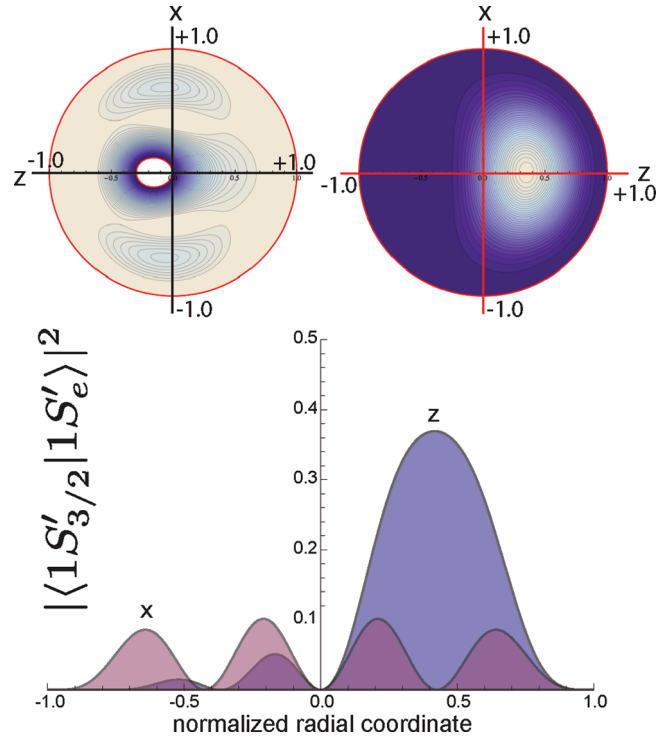

FIGURE 4. Normalized probability densities for hole (left) and electron (right) wavefunctions perturbed by a point (negative) charge positioned at −1 nm from the QD surface along the z-axis. The lower panel shows overlap integrals of the perturbed wavefunctions along the z- (blue) and x- (red) axes, from which we estimate a polarization ratio of ~3:1.

DOI: 10.1021/nl1001789 | *Nano Lett.* **XXXX,** *xxx,* 000–000

tion can be understood from a simple electrostatics argument in which the presence of a fixed charge polarizes the electron/hole wavefunction - in addition to the change in recombination energy, the extent of that wavefunction polarization defines both the total oscillator strength and polarization properties. It is interesting to point out that unlike atomic or molecular transitions that accommodate angular momentum conservation via changes in orbital symmetry, light absorption/emission in quantum dots is mediated through electron−hole spin creation/annihilation thus the envelope wavefunctions for electron and holes conserve orbital symmetry.[30] In the absence of any shape or electronic perturbation, this gives rise to the so-called 2D degenerate dipole characteristics of band-edge luminescence from quantum dots. More specifically, the optical transitions in the plane perpendicular to the *c*-axis of the QD involve dipole transitions $<1S_e|\mu|1S_{3/2,M=\pm 3/2,\pm 1/2}>$ driven by right and left circular polarization respectively with equal probability.[27] For the perturbed wavefunctions, transition dipole matrix elements of the form $<1S'_e|e\cdot z|1S'_{3/2,M=\pm 3/2,\pm 1/2}>$ are nonzero thus contributing to a linear polarization in emission along the *z*-axis. Additionally, we can look simply at the overlap functions $|<1S'_e|1S'_{3/2,M=\pm 3/2,\pm 1/2}>|^2\, r^2\, dr$ along the "*z*-" and "*x*-" axes. From this, we estimate a polarization ratio of about 3:1.

Conclusion. In conclusion, we have demonstrated large spectral shifts in the QD band-edge luminescence from single CdSe/OPV nanoparticles that are controlled externally by modulation of the excitation laser polarization. Supported by perturbation calculations of the magnitude of the Stark shift and resulting change in oscillator strength in the quantum dot core, these results provide compelling evidence for DC Stark effect mechanism underlying the observation of both a linear transition dipole moment and spectral shifts. We note here that the above analysis is based on a model involving the interaction of only one polariton with the quantum dot core. In reality, the interactions between ligands and the QD in single nanostructures is more complicated, and a full treatment would require consideration of multiple, distributed ligands. Computational approaches to this problem are a matter for further investigation. These results suggest that single QDs can act as sensitive local probes of charge migration and can be useful in both quantum dot solar cell and charge transport membranes applications.

Acknowledgment. Support from U.S. Department of Energy, Basic Energy Sciences (DE-FG02-05ER15965) is gratefully acknowledged. We would also like to acknowledge partial support from the National Science Foundation (NSF) Center for Chemical Innovation (CHE-0739227). P.K.S. acknowledges support from NSF-CHE 0750365; M.D.B. and T.E. acknowledge support from the "Polymer-based Materials for Harvesting Solar Energy" and the Energy Frontier Research Center funded by the U.S. Department of Energy under award number DE-SC0001087.

Supporting Information Available. Details of sample preparation, single particle spectral dynamics and statistics, and orientational fitting routines are included. This material is available free of charge via the Internet at http://pubs.acs.org.

REFERENCES AND NOTES

(1) Htoon, H.; Furis, M.; Crooker, S. A.; Jeong, S.; Klimov, V. I. *Phys. Rev. B* **2008**, *77* (3), 035328.
(2) Hu, J. T.; Li, L. S.; Yang, W. D.; Manna, L.; Wang, L. W.; Alivisatos, A. P. *Science* **2001**, *292* (5524), 2060–2063.
(3) Hammer, N. I.; Early, K. T.; Sill, K.; Odoi, M. Y.; Emrick, T.; Barnes, M. D. *J. Phys. Chem. B* **2006**, *110* (29), 14167–14171.
(4) Antelman, J.; Ebenstein, Y.; Dertinger, T.; Michalet, X.; Weiss, S. *J. Phys. Chem. C* **2009**, *113* (27), 11541–11545.
(5) Hohng, S.; Ha, T. *J. Am. Chem. Soc.* **2004**, *126* (5), 1324–1325.
(6) Milliron, D. J.; Alivisatos, A. P.; Pitois, C.; Edder, C.; Frechet, J. M. J. *Adv. Mater.* **2003**, *15* (1), 58–61.
(7) Odoi, M. Y.; Hammer, N. I.; Sill, K.; Emrick, T.; Barnes, M. D. *J. Am. Chem. Soc.* **2006**, *128* (11), 3506–3507.
(8) Odoi, M. Y.; Early, K. T.; Tangirala, R.; Sudeep, P. K.; Emrick, T.; Barnes, M. D. *J. Phys. Chem. C* **2009**, *113* (31), 13462–13465.
(9) Early, K. T.; McCarthy, K. D.; Odoi, M. Y.; Sudeep, P. K.; Emrick, T.; Barnes, M. D. *ACS Nano* **2009**, *3* (2), 453–461.
(10) Sudeep, P. K.; Early, K. T.; McCarthy, K. D.; Odoi, M. Y.; Barnes, M. D.; Emrick, T. *J. Am. Chem. Soc.* **2008**, *130* (8), 2384–2385.
(11) Jung, C.; Hellriegel, C.; Platschek, B.; Wohrle, D.; Bein, T.; Michaelis, J.; Brauchle, C. *J. Am. Chem. Soc.* **2007**, *129* (17), 5570–5579.
(12) Bartko, A. P.; Dickson, R. M. *J. Phys. Chem. B* **1999**, *103* (51), 11237–11241.
(13) Bohmer, M.; Enderlein, J. *J. Opt. Soc. Am. B* **2003**, *20* (3), 554–559.
(14) Patra, D.; Gregor, I.; Enderlein, J. *J. Phys. Chem. A* **2004**, *108* (33), 6836–6841.
(15) Ha, T.; Laurence, T. A.; Chemla, D. S.; Weiss, S. *J. Phys. Chem. B* **1999**, *103* (33), 6839–6850.
(16) Empedocles, S. A.; Bawendi, M. G. *Science* **1997**, *278* (5346), 2114–2117.
(17) Biadala, L.; Louyer, Y.; Tamarat, P.; Lounis, B. *Phys. Rev. Lett.* **2009**, *103* (3), 37404.
(18) Neuhauser, R. G.; Shimizu, K. T.; Woo, W. K.; Empedocles, S. A.; Bawendi, M. G. *Phys. Rev. Lett.* **2000**, *85* (15), 3301–3304.
(19) Shen, Y. M.; Pang, L.; Fainman, Y.; Griswold, M.; Yang, S.; Butov, L. V.; Sham, L. J. *Phys. Rev. B* **2007**, *76* (8), No. 085312.
(20) Lee, S. F.; Osborne, M. A. *ChemPhysChem* **2009**, *10* (13), 2174–2191.
(21) van Sark, W. G. J. H. M.; Frederix, P. L. T. M.; Bol, A. A.; Gerritsen, H. C.; Meijerink, A. *ChemPhysChem* **2002**, *3* (10), 871–879.
(22) Empedocles, S. A.; Norris, D. J.; Bawendi, M. G. *Phys. Rev. Lett.* **1996**, *77* (18), 3873–3876.
(23) Empedocles, S. A.; Neuhauser, R.; Shimizu, K.; Bawendi, M. G. *Adv. Mater.* **1999**, *11* (15), 1243–1256.
(24) Campbell, I. H.; Hagler, T. W.; Smith, D. L.; Ferraris, J. P. *Phys. Rev. Lett.* **1996**, *76* (11), 1900–1903.
(25) Greenham, N. C.; Peng, X. G.; Alivisatos, A. P. *Phys. Rev. B* **1996**, *54* (24), 17628–17637.
(26) Ginger, D. S.; Greenham, N. C. *Synth. Met.* **1999**, *101* (1−3), 425–428.
(27) Efros, A. L. *Phys. Rev. B* **1992**, *46* (12), 7448–7458.
(28) Wang, L. W. *J. Phys. Chem. B* **2001**, *105* (12), 2360–2364.
(29) Wang, L. W.; Zunger, A. *Phys. Rev. B* **1996**, *53* (15), 9579–9582.
(30) Efros, A. L.; Rodina, A. V. *Phys. Rev. B* **1993**, *47* (15), 10005–10007.

DOI: 10.1021/nl1001789 | *Nano Lett.* **XXXX,** *xxx,* 000–000